Development 130, 3137-3146
© 2003 The Company of Biologists Ltd
doi:10.1242/dev.00549

Arabidopsis CROOKED encodes for the smallest subunit of the ARP2/3 complex and controls cell shape by region specific fine F-actin formation

Jaideep Mathur*, Neeta Mathur, Victor Kirik, Birgit Kernebeck, Bhylahalli Purushottam Srinivas and Martin Hülskamp*

Botanical Institute III, University of Köln, Gyrhofstrasse 15, Köln, D-50931, Germany
*Authors for correspondence (e mail: jaideep.mathur@uni-koeln.de and martin.huelskamp@uni-koeln.de)

Accepted 15 April 2003

SUMMARY

The generation of a specific cell shape requires differential growth, whereby specific regions of the cell expand more relative to others. The *Arabidopsis crooked* mutant exhibits aberrant cell shapes that develop because of mis-directed expansion, especially during a rapid growth phase. GFP-aided visualization of the F-actin cytoskeleton and the behavior of subcellular organelles in different cell-types in *crooked* and wild-type *Arabidopsis* revealed that localized expansion is promoted in cellular regions with fine F-actin arrays but is restricted in areas that maintain dense F-actin. This suggested that a spatiotemporal distinction between fine versus dense F-actin in a growing cell could determine the final shape of the cell. *CROOKED* was molecularly identified as the plant homolog of ARPC5, the smallest sub-unit of the ARP2/3 complex that in other organisms is renowned for its role in creating dendritic arrays of fine F-actin. Rescue of *crooked* phenotype by the human ortholog provides the first molecular evidence for the presence and functional conservation of the complex in higher plants. Our cell-biological and molecular characterization of *CROOKED* suggests a general actin-based mechanism for regulating differential growth and generating cell shape diversity.

Key words: Cytoskeleton, ARP2/3-complex, Actin, Trichomes, Morphogenesis

INTRODUCTION

Differential growth determines the final shape of a cell. In plants, although the multi-step process of general growth involving the spatiotemporal targeted exocytosis of vesicles to the cell exterior has been well dissected (Hawes et al., 1999), the specific intracellular conditions required for differential growth are not well defined. It is known that the actin cytoskeleton is intimately involved during growth-site selection, the subsequent mobilization of the endo-membrane-secretory system as well as in the final step of delivering exocytic vesicles to the selected site (Hepler et al., 2001; Qualmann et al., 2000). Consistent with these roles a general interference with the polymerization of globular (G) actin into its filamentous (F) actin form during plant development leads to near cessation of intracellular motility and results in short, unexpanded and frequently deformed cells (Baluska et al., 2001; Mathur and Hülskamp, 2002). What is not known is how certain regions of the cell are excluded from the general growth process while others carry out localized growth.

Two recent studies have suggested that only certain actin configurations might be favorable for triggering local growth. It was observed in tip-growing root hairs that unstable (very dynamic) actin is essential for localized expansion (Ketelaar et al., 2003) and that cell-surface expansion caused by overexpression of the general actin-cytoskeleton regulator ROP (a plant Rho-like-GTPase) correlates with an overall increase in fine filamentous (F-) actin (Fu et al., 2002). If only fine F-actin is conducive for local growth, would a denser F-actin configuration hinder growth? Furthermore, what is the molecular identity of the factor responsible for the creation of fine F-actin?

We have approached these questions through the cell-biological and molecular analysis of *crooked*, an *Arabidopsis* mutant belonging to the *distorted* class, that characteristically exhibits expansion-related defects of short, irregularly shaped trichome cells (Hülskamp et al., 1994). Actin inhibitors phenocopy the *dis* mutants and the F-actin cytoskeleton in mutant trichomes is usually aberrant (Mathur et al., 1999; Szymanski et al., 1999). We show that the development of aberrant shapes in different cell types in *crooked* is linked to the progressive accumulation of dense actin in atypical intracellular locations. Furthermore, actin organization and localized expansion in *crooked* cells correlates with the behavior and distribution of subcellular organelles and expansion is promoted only in those cellular regions that possess fine F-actin, whereas it is severely restricted in areas with dense F-actin accumulations. Subsequent molecular identification of *CROOKED* showed it to be the plant ortholog of ARPC5 (Cooper et al., 2001), the smallest subunit of a conserved actin polymerization enhancer, the ARP2/3 complex, that in other organisms is required for creating fine dendritic arrays of F-actin (Machesky and Gould, 1999; Svitkina and Borisy, 1999). Our combined cell-biological and

molecular characterization of *CROOKED*, and the comparative data from wild-type *Arabidopsis* suggest that the local density of F-actin can either permit or limit exocytic vesicles from reaching the plasma membrane for their final assimilation step that is required for localized expansion and differential growth.

MATERIALS AND METHODS

Plant materials and growth conditions

The *crooked* mutant is in the Landsberg *erecta* background (wild type) and was isolated in an EMS mutagenesis screen (Hülskamp et al., 1994). Different transgenes, *p35S-GFP-mTalin* (Kost et al., 1998), *p35S-ERD2-GFP* (Boevink et al., 1998) and *p35S-YFP-peroxisome* (Mathur et al., 2002), were introduced into the wild-type and *crooked* plants by genetic crossing or *Agrobacterium tumefaciens* (strain GV3101) mediated floral dip transformation (Clough and Bent, 1998). T1 plants were screened on MS medium (Murashige and Skoog, 1962) selection plates containing 25 μg/ml Hygromycin B. Phenotypic and cell-biological characterization were carried out on both in vitro (MS salts, 3% sucrose, 1% Phytagar; 23°C, 16 hours daylight/8 hours dark) and soil grown plants (ambient light/dark conditions). Experiments challenging cell growth were carried out by germinating wild-type and mutant seeds in the dark (23°C) for 7-10 days before opening the plates for phenotype characterization. Root hair cells were challenged to elongate by tilting plates ~20° from the vertical such that roots and hair cells projected out into an airy environment before reaching the agar medium.

Transient expression of DNA in seedlings

The identification of a positive BAC clone capable of rescuing the *crooked* phenotype, as well as initial testing of the different cDNA/genomic and GFP-linked constructs, was carried out through transient expression assays. Seeds were sown in the center of plates containing MS medium and used when the seedlings were 7-9 days old (first leaf primordia just visible). The DNA (cDNA/genomic, BAC) being tested was mixed with GFP-mTalin in a 1:1 ratio (ca. 500 ng DNA/μl), precipitated around 1 μm diameter gold particles (BioRad, Hercules, CA) following the manufacturer's directions, loaded onto carrier membranes and shot into the plants at 1100 psi Helium pressure under a vacuum of 25 inches of Hg, using a PDS-1000/Helium driven Biolistic delivery apparatus (BioRad). Plants were screened for green fluorescence under FITC filter illumination after 16 hours and the development of trichome/other cells expressing the shot-DNA followed for up to 48 hours. The addition of GFP-mTalin ensured visualization of the shot cell and was not required when other fluorescent fusion constructs such as *p35 S-YFP-mTalin* and *p35S-ERD2-GFP* were used.

Microscopy and image processing

Agarose impressions of epidermal surfaces were prepared as described (Mathur and Koncz, 1997). Light and fluorescence microscopy was carried out on a LEICA-DMRE microscope equipped with a high resolution KY-F70 3-CCD JVC camera and a frame grabbing DISKUS software (DISKUS, Technisches Büro, Königswinter). Lime lapse movies were created using DISKUS software or the Leica CLSM software and later processed using the Quick Time 5.0 movie software. Velocity measurements for cytoplasmic streaming, peroxisomes and Golgi bodies were taken as described earlier (Mathur et al., 2002) on a minimum of 25 trichomes and root-hair cells each. For confocal laser scanning microscopy plants were grown as described (Mathur et al., 1999). The descriptions provided here were obtained on 25 (each observation) randomly selected wild-type and transgenic plants. A spectrophotometric CLSM (Leica TCS-SP2) was used for visualizing EGFP, and discriminating between EYFP/EGFP using the settings as described (Mathur et al., 2002). Images were sized, processed for brightness/contrast and CMYK alterations using the Adobe Photoshop 6.0 software.

Molecular techniques

The *crooked* gene was isolated following a candidate gene approach based on its map position (chromosome 4) and a cell biological characterization. The putative actin polymerization factor was identified (At4g01710 from contig t15b16) in the MIPS *Arabidopsis* database (http://mips.gsf.de/cgi-bin/proj/thal/). Attempts to isolate the crooked cDNA were based on the annotated sequence available for gene (At4g01710; MIPS). After the web publication of a full-length cDNA for At4g01710 gene (RAFL06-77-B13; Resource no. pda03657; NCBI Accession Number AY052191; http://pfgweb.gsc.riken.go.jp/index.html), a primer set (JM364R GGAATGATGGATCAAACGGT-GTTGATGGTATCAGTAAG and JM365F GAGAGAAAGATCGA-ATCGAAGAATGGCAGAATT) was designed to provide a 515 bp clone from a cDNA library DNA generated from 25-day-old, soil grown plants of *Arabidopsis thaliana* (ecotype Landsberg erecta) using standard procedure (Sambrook and Russel, 2001). The transcriptional start site for At4g01710 was determined by RNA ligase-mediated rapid amplification of 5′ cDNA ends (RLM-RACE) carried out using the Gene Racer kit (Cat. No. L1500-01; Invitrogen) according to the manufacturer's instructions. The genomic clone (ATG to TGA) of At4g01710 was PCR-amplified from genomic DNA extracted from wild-type and mutant plants (PCR primers: JM 64F GTACTCAGGATCCTCGGCTTATGTCTCCGG and JM65R ATAC-ATAAGAGGGAGCTCAATGATGGATCA). Details of other primers and PCR conditions are available on request. The genomic and cDNA fragments were sub-cloned into a pGEM-T-easy vector (Promega), sequenced on an ABI-prism sequencer and finally cloned into a pCAMBIA 1300 binary vector (accession number AF234296) under the control of a cauliflower mosaic virus promoter (CaMV p35S), or a trichome specific *GLABRA2* promoter (Szymanski et al., 1998) for plant transformation. DNA and protein sequence homology searches were carried out using the respective BLAST programs (Altschul et al., 1997). Amino acid alignments were carried out using the Clustal-W multiple sequence alignment algorithm (http://www.ch.embnet.org/).

RESULTS

CROOKED is specifically required during rapid cell expansion

The *crooked* mutant displays random expansion in many polarized cell types during rapid growth (Fig. 1). During trichome development, distortions accrue during the rapid expansion phase that follows the initiation of branch points. As a result, the highly co-aligned orientation of branches with respect to the main leaf axis becomes randomized. Trichomes in *crooked* are short (150-350 μm compared to 400-500 μm tall in wild type Fig. 1A) with the branches remaining as stumpy, unextended spikes (Fig. 1B). Polarized expansion of hypocotyl (cell length wild type 250±50 μm; mutant 130±45 μm) is reduced by a factor of 1.5-2.7 (Fig. 1C,D). Stomatal complexes that are typically found in wild type are often missing in the *crooked* mutant (Fig. 1E,F). Cells of expanding cotyledons are smaller (wild type 500±65 μm; mutant 170±60 μm along the longest axis; n=100) and frequently devoid of lobes (Fig. 1G,H), which are believed to result from localized cell expansion during epidermal cell differentiation (Frank and Smith, 2002). The defects become even more pronounced when cells are challenged to expand faster. Under low-light conditions, hypocotyl elongation is greatly reduced in *crooked* (total length; wild type: 2.8±0.7 cm; *crooked*: 1.3±0.6 cm;

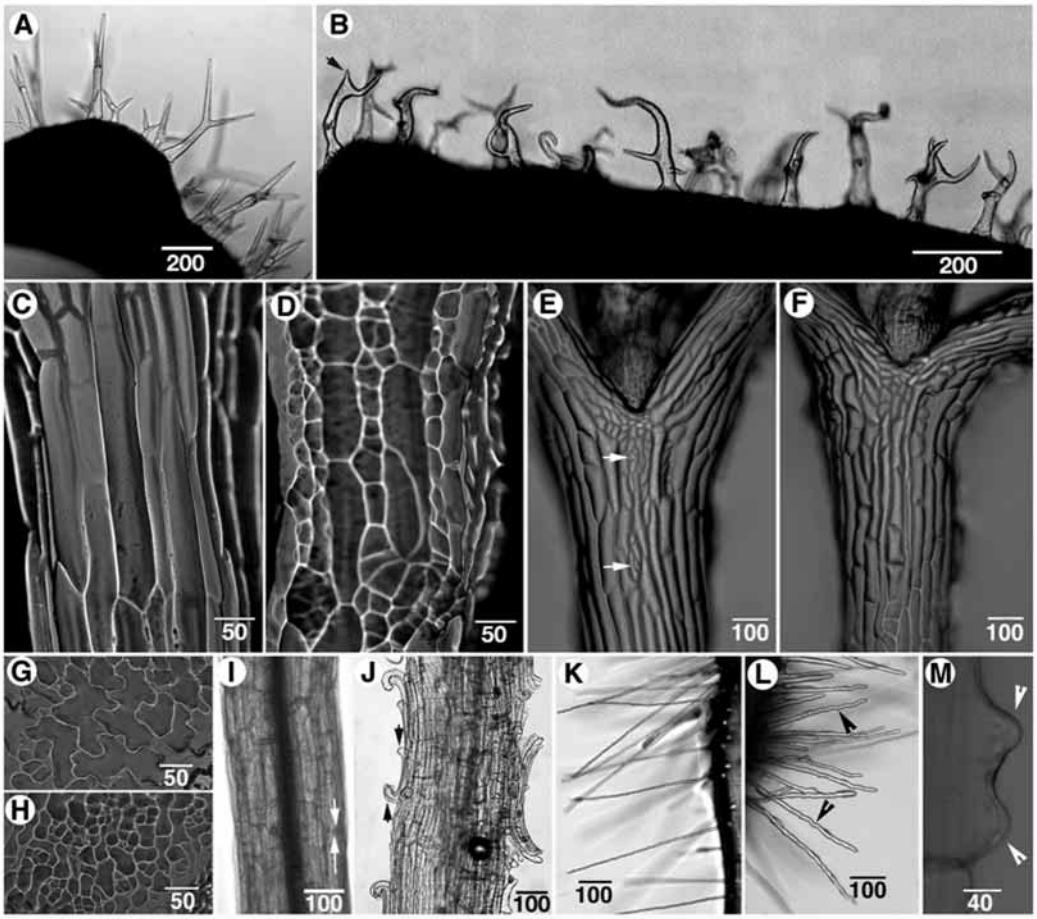

Fig. 1. A comparison of different cell types in *Arabidopsis* (ecotype Landsberg *erecta*) wild type and the *crooked* mutant. (A) Two or three branched, stellate wild-type trichomes. (B) Randomly shaped, distorted trichomes in *crooked* with unextended branches (arrow) located in aberrant positions. (C) Typically elongated cells occupy the mid-zone of wild-type hypocotyl in 10-day-old seedlings. (D) The hypocotyl mid-zone of 10-day-old *crooked* seedlings shows radially expanded cells and a lack of the file arrangement observed in wild type. (E) A hypocotyl of 7-day-old wild-type seedling displays clearly differentiated stomatal complexes (arrows). (F) A hypocotyl of a 7-day-old *crooked* seedling does not possess stomatal complexes in the characteristic regions. (G) The typical epidermal surface of expanding wild-type cotyledons patterned into a jigsaw puzzle shape through cell-lobing. (H) Cotyledon-cells in *crooked* are less expanded compared with the wild type and are impaired in lobe formation. (I) Hypocotyl of wild-type seedling challenged to elongate rapidly by growing in dark for 7 days show a regular arrangement of cell files with each cell firmly in contact with its neighbors (arrows at cell junction). (J) The hypocotyl of a *crooked* seedling challenged into rapid elongation became scruffy as cells broke contact with their neighbors along the long axis and curled outwards (arrows) to leave gaps in the epidermis. (K) Wild-type root hairs are straight, tubular and can elongate up to 1 mm. (L) Root hairs in *crooked* are 1.5- to 2-fold thicker than wild-type hairs, are sinuous (arrowheads) and can display varying diameters along their length. (M) A single trichoblast in *crooked* showing aberrant development of two root-hair initials (arrowheads). Numbers given below scale bars are in μm.

n=25). The hypocotyl surface is scruffy, resulting from cells becoming unlinked from each other, primarily along the longitudinal growth axis, and consequently curling out of the epidermal plane (Fig. 1I,J). Similarly, root hairs challenged into rapid growth by tilting the plates downwards (20° from the vertical) remain either short and stunted (wild type 500-960 μm; *crooked* 180-250 μm long; *n*=150) or elongate up to 600 μm but exhibit varying degrees of waviness (Fig. 1K,L). Contrary to the wild-type situation, nearly 13% (*n*=100) of the observed trichoblast cells in *crooked* develop additional tip-growing regions to produce more than one root hair from the same cell (Fig. 1M).

On the basis of the above observations we concluded that the *CROOKED* gene product is required during rapid cell expansion. As the actin cytoskeleton is known to be essential for cell expansion (Baluska et al., 2001; Mathur and Hülskamp, 2002), we compared the F-actin organization in wild-type cells with that in *crooked* cells.

F-actin configuration is aberrant in *crooked* and mis-localizes areas of differential expansion

F-actin was visualized in living cells using plants expressing the GFP-mTalin transgene that has been shown to specifically bind to filamentous-actin with a high affinity (McKann and Craig, 1997; Kost et al., 2000). However, during the early stages of development, both wild-type and *crooked* trichomes displayed a general green fluorescence where it was not possible to discriminate between fine and dense actin (data not shown). Our observations on the actin cytoskeleton started soon after the formation of branch initials when the trichome cell enters a rapid expansion phase (Szymanski et al., 1999). In wild-type trichomes, the cortical regions were enmeshed in very fine F-actin, whereas dense F-actin accumulation was observed only in small domains at the branch tips, in the region of branch-bifurcation (Fig. 2A), and as a few adherent actin patches in elongating branches. With further expansion, the cortical fine actin filaments became relatively diffuse and difficult to resolve, actin patches on the sides of branches disappeared and well-defined F-actin cables became prominent (Fig. 2A). A wild-type trichome cell with fully extended branches thus displayed prominent longitudinally aligned subcortical F-actin cables, connecting together in the dense actin patches that are maintained at branch tips and branch junctions (Fig. 2B). F-actin organization in *crooked* trichomes

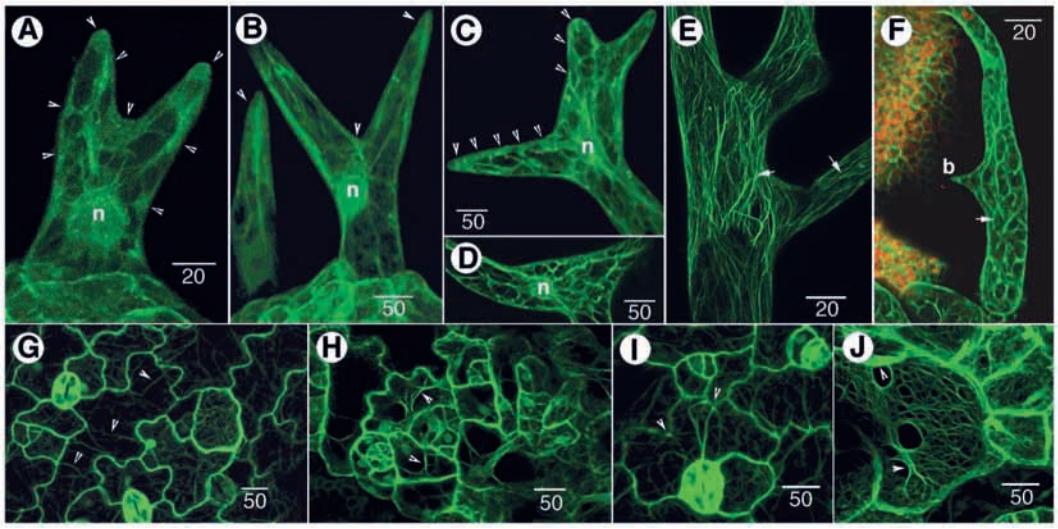

Fig. 2. GFP-mTalin aided visu*aliza*tion *o*f F-actin organization in trichome and cotyledon-epidermal cells of wild-type *Arabidopsis* and *crooked* mutant (n, nucleus; numbers given below scale bars are in μm). (A) A wild-type trichome that has initiated branches and is ready to embark on a rapid expansion phase. Trichomes in *crooked* exhibit a similar F-actin organization at this stage, with major actin accumulations as shown (arrowheads). (B) Wild-type trichomes where branches have started extending maintain dense F-actin at the tips and junctions of branches (arrowheads), while elongated F-actin cables connecting regions of dense actin start to become prominent. (C) A *crooked* trichome at a stage comparable with that of wild type in B displays an increase in dense F-actin bundles throughout the cell, resulting in more intracellular areas being covered by dense actin (arrowheads). Note that the cell starts thickening around its mid region while the uppermost branch maintains a rounded tip, suggesting less extension of the flanks. (D) A slightly more advanced stage of development in a *crooked* trichome shows massive actin bundling and the organization of a characteristic wide-polygonal mesh. Note that in A-D, while dense actin can be easily visualized, areas with very fine and difficult to resolve F-actin meshwork are only visible as a diffuse green fluorescence. (E) A region of a mature wild-type trichome displaying predominantly longitudinally oriented (arrows) F-actin bundles. (F) A mature *crooked* trichome with predominantly transversely arranged, cross-connected, thick actin bundles appears subdivided into numerous polygonal compartments (arrowhead). Note that the *crooked* trichome has not been able to expand well and one of the branches 'b' is visible as a short unextended spike. (G) Expanding wild-type cotyledon epidermis displaying the typical puzzle-shaped cells with prominent lobes. A fine, diffuse cortical F-actin and thick F-actin cables (e.g. arrowheads) connecting strategic points within each cell are seen. (H) A comparative view of the cotyledon epidermis in *crooked* shows thickly bundled F-actin (arrowheads) and impaired lobe formation. (I) A higher magnification of wild-type cotyledon epidermal cells shows the occurrence of dense actin specifically at lobe sinuses (e.g. arrowheads), while other areas of the cell possess relatively finer F-actin organization. (J) A cotyledon epidermal cell in *crooked* with no lobes displays a general distribution of bundled actin. The arrowheads indicate thicker bundles.

started essentially in a manner similar to the wild type, with fine cortical F-actin and dense actin configurations at the tips and junction and sides of branches (Fig. 2A). However, in contrast to the wild type, actin patches did not disappear with progressing age of the cell but instead became more prominent through increased actin accumulation (Fig. 2C). In addition, instead of developing into the extended actin cables typical to the wild type, the F-actin in *crooked* (Fig. 2C-E) became organized into numerous, thick, transversely linked actin bundles and produced a characteristic, wide-polygonal meshwork (Fig. 2D,F). Dense actin bundling in many *crooked* trichomes did not extend throughout the cell and left random pockets where fine cortical F-actin could still be observed. Though *crooked* trichomes never displayed the diffuse cortical F-actin state shown by wild-type trichomes, regions containing the relatively fine cortical actin expanded more when compared with areas filled with dense actin. Trichomes in *crooked* trichomes consequently showed randomly localized regions of expansion (with fine F-actin) and non-expansion (with bundled F-actin).

The lobed, jigsaw puzzle-shaped epidermal cells in expanding wild-type cotyledons displayed fine cortical F-actin and thick sub-cortical F-actin cables connected to points at lobe sinuses (Fig. 2G). Smaller actin bundles frequently linked the two expanding sides of a lobe. By contrast, 45±12% (n=100) of the cotyledon epidermal cells in *crooked* were malformed and did not develop lobes (Fig. 2H), These cells in general had more actin bundles when compared with the wild type (Fig. 2H-J) and, depending upon the density of F-actin, could either be very small, abnormally elongated along one axis or slightly expanded and irregularly lobed. In mutant cells where lobe formation did take place, both the cortical and subcortical F-actin organization were similar to the wild type. Hypocotyl cells in wild type exhibited a fine, cortical F-actin mesh and longitudinally stretching subcortical cables connecting the relatively actin-rich cell ends (Fig. 3A). In *crooked*, in 67±13% (n=150) of cells, F-actin strands clumped together into thick transversely connected bundles (Fig. 3B). When challenged into rapid growth, wild-type hypocotyl cells elongated and maintained their fine, predominantly longitudinal oriented, F-actin meshwork (Fig. 3C) whereas *crooked* cells responded by developing increased actin bundling (Fig. 3D). Actin bundling in mutant cells extended either throughout the cell and coincided with a short cell size or was limited to small regions at the cell ends. Unequal expansion subsequently produced small bulges at such cell ends (Fig. 3E-G). Nearly 65±8% (n=430) of mutant hypocotyl cells thus curled upwards, tearing considerable gaps in the epidermal layer (Fig. 3F,G). In these cells, actin bundling always preceded the actual cell separation. In addition, root hairs, which are known to extend exclusively by tip growth (Geitmann and Emons, 2000), in *crooked* exhibited a strict correlation of fine F-actin with growing and

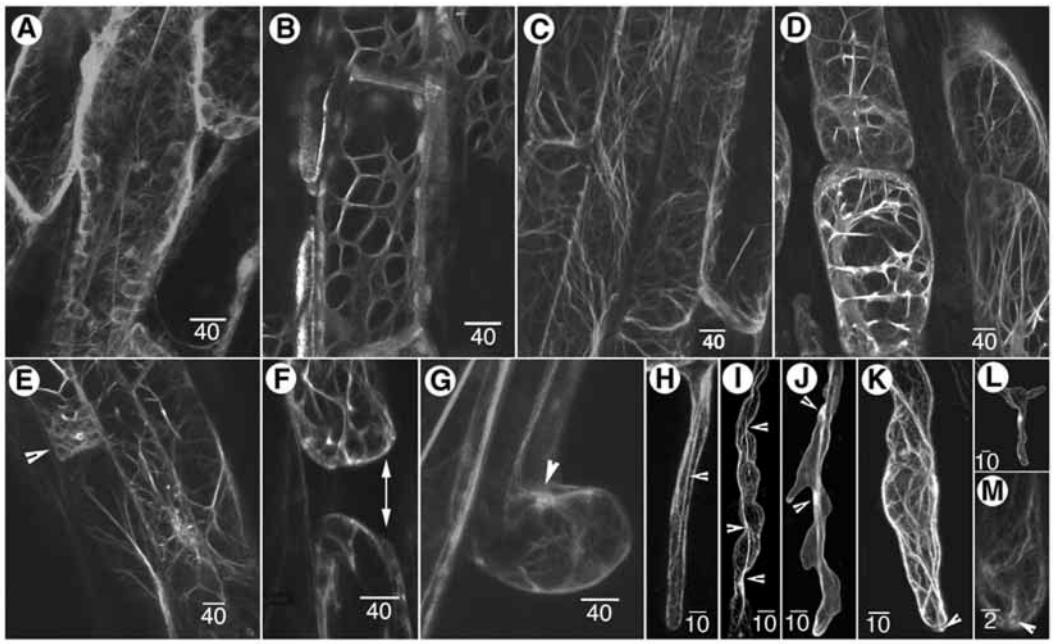

Fig. 3. F-actin organization in expanding hypocotyl and root hair cells in wild-type *Arabidopsis* and *crooked* mutant. (Numbers given below scale bars are in μm.) (A) Wild-type hypocotyl cells displaying fine cortical F-actin mesh and longitudinally running subcortical F-actin cables connecting the cell ends. (B) Hypocotyl cells in *crooked* with thick, transversely linked F-actin bundles. (C) Dark grown, elongated wild-type hypocotyl cells with fine F-actin meshwork. (D) Aberrant actin bundling in *crooked* hypocotyl cells challenged to elongate rapidly. (E) Dark-grown *crooked* hypocotyl cells, a cell with one end displaying actin bundles (arrowhead). (F) Actin bundles at a *crooked* cell end mislocalize growth and create less elongating cells with bulged ends. Note that the two contiguous cells now break contact, leaving a gap in the hypocotyl epidermis (double-headed arrow). (G) A single hypocotyl epidermis cell in *crooked* curls up. Note that the site of dense actin (arrowhead) coincides with a less growing region whereas the outer more expanded curve has a thinner layer of actin. (H) A wild-type root hair with long actin bundles that stop just before the apex. (I,J) Sinuous root hairs from *crooked* with longitudinally extended actin bundles. Note that the regions where the actin bundle contacts and obscures the plasma membrane do not expand (arrowheads), whereas regions free from the bundle expand more. (K) A swollen root hair from *crooked* is filled with actin-bundles extending all the way to the tip (arrowhead). (L) A branched *crooked* root hair creates another region for tip growth. (M) Magnified view of the tip region in L shows dense actin at the tip (arrowhead), suggesting that inhibition of the growth of the original tip region (caused by dense actin) resulted in a new tip being formed.

bundled F-actin with non-growing regions. Short *crooked* root hairs (maximum width/length ratio=1:30 compared with the nearly uniform 1:70 ratio in wild type Fig. 3H-K) displayed actin bundling up to the very tip that in the wild type would normally contain only fine F-actin. Root hairs with varying diameter along their length (range 9-20 μm) and a wavy appearance displayed patches of bundled actin at regions of constriction alternating with expanded regions containing fine-actin (arrows Fig. 3I,J). Some extending root hairs initiated fresh tips (Fig. 3L) after the accumulation of dense actin at the original tip region (Fig. 3M).

A comparison of the F-actin organization between wild type and *crooked* thus revealed bundled actin to be strictly localized to non-expanding regions, while expanding regions always possessed fine F-actin. The finding that the *CROOKED* gene product appeared to be essential for creating/maintaining a fine F-actin organization raised the question of how the loose versus dense actin configurations affected intracellular organization and regional transport processes, the coordination of which is essential for growth.

We focused our analysis on visualizing the general cytoplasmic streaming and the endo-membrane system, the mobility of which is known to depend on the actin cytoskeleton (Williamson, 1993; Boevink et al., 1998).

Cytoplasmic organization and behavior of Golgi bodies exhibits regional differences in *crooked*

The correlation of expanding regions with fine F-actin and non-expanding regions with dense F-actin in *crooked* cells suggested that during their development the dynamics and distribution of organelles might also be affected in a region-specific manner. In general, wild-type trichomes displayed a longitudinally oriented cytoplasmic organization with transversely linked cytoplasmic strands occurring mainly in the stalk region and spanning the large central vacuole. The cytoplasmic streaming in wild-type trichomes occurred at an average velocity of 0.8±0.3 μm/second. In *crooked* trichomes, the cytoplasmic organization in expanded regions was similar to the wild type though the velocity of cytoplasmic streaming was reduced to 0.6±0.3 μm/second (n=25). However, cytoplasmic strands became thick and transversely linked in non-expanded areas of *crooked* trichomes whereas cytoplasmic streaming became reduced to 0.3-0.5 μm/second in these areas. This was independently confirmed by analyzing the saltatory movement of peroxisomes, known to occur along F-actin tracks (Mathur et al., 2002). In well-expanded regions of *crooked* trichomes, peroxisome motility was found to be comparable with that of the wild type (average velocity 0.9±0.2 μm/second; n=25) but was reduced by up to 15-fold in unexpanded areas. Taken together, these data indicate that actin-dependent organelle movement was moderately impaired but not blocked in expanding regions with fine F-actin, whereas organelles were trapped into near immobility in areas with dense actin.

We focused our further analysis on Golgi bodies, which are known to track along F-actin strands (Boevink et al., 1998; Nebenführ et al., 1999) and are suggested to have a direct bearing on localized growth through its processing and release

of exocytosis-competent vesicles (Miller et al., 1999). The stably expressed ERD2-GFP marker (Boevink et al., 1998) that we used, predominantly labeled the Golgi stacks in actively growing *Arabidopsis* cells (Fig. 4). In wild-type trichomes, 0.6-1.0 μm oblong to spherical Golgi bodies were found regularly distributed and moved with velocities ranging from 0.2 to 1.8 μm/seconds (n=150). As described for other plant cells (Boevink et al., 1998; Nebenführ et al., 1999), both short oscillatory movements, as well as long-range saltations are observed. Areas with major accumulation of Golgi bodies were not observed in growing wild-type trichomes, although Golgi bodies did exhibit a tendency to slow down within the narrow confines of extending branches (Fig. 4A). By contrast, both the number and size of Golgi bodies was found to be increased by two- to fivefold in *crooked* trichomes (Fig. 4A,B) with certain regions showing accumulations of up to 15 individual, 1-3 μm long, Golgi bodies (Fig. 4B,C). Paradoxically, despite the regional increase in the Golgi bodies, these regions corresponded to non-expanded areas of *crooked* trichomes, suggesting that the release and transport of Golgi-processed vesicles might be affected. Transient co-expression of YFP-mTalin (labeled F-actin) and ERD2-GFP markers followed by their confocal spectral separation allowed simultaneous visualization of actin and Golgi bodies in developing *crooked* trichome cells and confirmed the accumulation of Golgi bodies within pockets of dense F-actin (Fig. 4D). More region-specific behavioral differences also became apparent; Golgi bodies in expanded regions of *crooked* trichomes moved singly or in pairs in a manner similar to the wild type, whereas those trapped in dense F-actin-filled non-expanded regions performed very short 1-3 μm oscillations. We assumed that fine F-actin had to be present in a cellular region for Golgi-processed vesicles to be released efficiently for their assimilation leading to local expansion.

CROOKED encodes the smallest subunit of an actin nucleating complex

The *CROOKED* gene was mapped to the chromosome 4 (B. Schwab, PhD Thesis, University of Tübingen, 2001). Based on our cell-biological characterization, candidate genes were cloned and tested for their ability to rescue the mutant *crooked* phenotype in transient assays. One gene At4g01710, annotated as a putative actin polymerization factor (APF; MIPS *Arabidopsis* data-base) rescued the mutant trichome phenotype completely. That this single copy gene represented *CROOKED* was confirmed by rescuing mutant plants with the corresponding genomic fragment containing 900 bp of the 5′ and 95 bp of the 3′ untranslated region. The exon-intron structure (Fig. 5A) and the transcription start site were determined by comparing the genomic DNA with RT-PCR-amplified cDNA fragments and RLM-RACE PCR, respectively. The *crooked*1-1 allele used contained a single point mutation at position 1040 at the splice donor site of the second exon that leads to premature splicing, a 35 bp deletion in exon 2 (Fig. 5B,C), and a frame shift resulting in a stop codon 129 bp downstream of the start codon (Fig. 5D). *CROOKED* expression was found in all organs analyzed through RT-PCR (Fig. 5E). The predicted CROOKED protein showed sequence similarity to ARPC5, the smallest 16 kDa subunit of the ARP2/3 complex known from other organisms (Welch et al., 1997) (Fig. 5F). The amino acid sequence identity ranged from 32% for humans to 23% for budding yeast (Fig. 5F).We tested the functional conservation of the subunit by expressing the human ARPC5 ortholog (Welch et al., 1997) under the control of a trichome specific *GLABRA2* promoter (Szymanski et al., 1998) in mutant plants. The *crooked* trichome phenotype was completely rescued to wild-type morphology with both the human and *Arabidopsis* cDNA in these experiments, indicating that the ARPC5 subunit is functionally conserved between humans and plants. As the highest area of homology displayed by the predicted CROOKED protein to other orthologs (Fig. 5F) occurs in the 3′ region, the mutant would contain only the first 44 amino acids of the native protein (Fig. 5D) and lack most of the relatively conserved region.

DISCUSSION

CROOKED is required for localized alterations in F-actin configuration required for differential growth

The final step in the general process of growth requires vesicles carrying plasma membrane and cell wall reinforcing materials

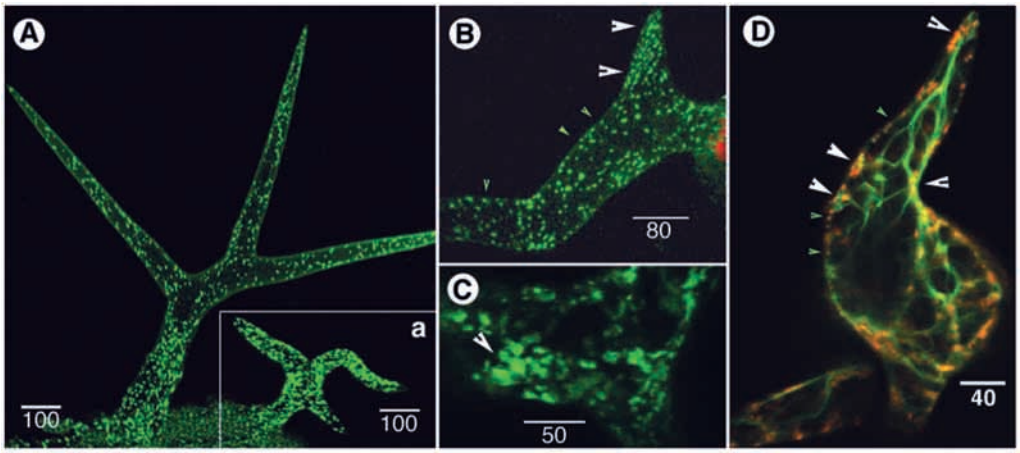

Fig. 4. Golgi-bodies in wild-type *Arabidopsis* and *crooked* cells. (A) Single wild-type and *crooked* 'a' trichomes of the same age, showing the differences in distribution and density of Golgi bodies. (B) Regional variation in distribution of Golgi bodies in a *crooked* trichome. The tip region has not expanded well but is densely packed with Golgi bodies (arrowheads). (C) Magnified view of a region exhibiting accumulation of Golgi bodies (arrowhead). (D) Co-visualization of F-actin bundles using YFP-mTalin fusion protein (green) and Golgi-bodies using ERD2-GFP label (red) in a *crooked* trichome shows that multiple Golgi bodies (such as those seen in C) are trapped in regions of dense actin (white arrowheads), whereas more loosely distributed, free Golgi bodies occur in expanded areas (green arrowheads).

to reach and deposit their cargo at target sites for assimilation (Foissner et al., 1996; Hawes et al., 1999; Miller et al., 1999). The generation of a specific cell shape, however, requires differential growth activity, whereby a specific region of the cell expands more than the others. This expanding region plausibly recruits more exocytic vesicles. Factors that create regional conditions for efficient release of vesicles therefore determine the final shape of a cell. The drug-based study of Ketelaar et al. (Ketelaar et al., 2003) has clearly demonstrated

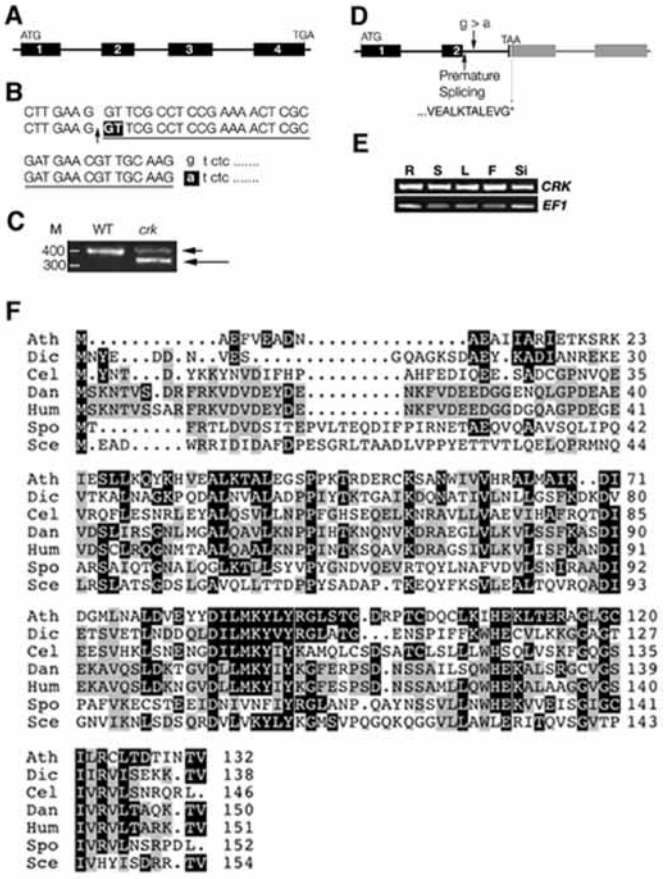

Fig. 5. Molecular details of the *Arabidopsis CROOKED* gene. (A) The exon-intron structure for At4g01710 (*CROOKED*) as determined by comparing the genomic DNA with RT-PCR-amplified cDNA fragments and RLM-RACE PCR, respectively. (B) The *crooked* mutant sequence contains a single point mutation (g>a) at the splice donor site, which leads to premature splicing (arrow) and a 35 bp deletion in exon 2 (nucleotides underlined). (C) RT-PCR using wild-type and *crooked* cDNA shows that the premature splicing produces a smaller transcript of 360 bp (large arrow) and a weak band (small arrow) corresponding to the 399 bp wild-type transcript. (D) The altered splice site predicts a frame shift resulting in a stop codon 129 bp downstream of the start site and a truncated amino acid sequence of only 44 residues (the last 12 shown). (E) Tissue-specific RT-PCR shows *CROOKED* to be ubiquitously expressed (R, root; S, inflorescence stem; L, leaves; F, flowers; Si, young siliques). The lower lane shows the elongation factor 1 transcript used as a loading control. (F) The predicted amino acid sequence for CROOKED aligned against ARPC5 subunit sequences from other organisms (Ath, *A. thaliana*; Dic, *D. discoideum* (31%); Cel, *C. elegans* (32%); Dan, *D. rerio* (29%); Hum, *H. sapiens* (32%); Spo, *S. pombe* (25%); Sce, *S. cerevisiae* (23%). Percentages (%) indicate amino acid identity (black); gray areas show similar amino acids.

that a localized occurrence of fine F-actin is conducive for vesicle release and promotes local expansion. Our cell-biological characterization of *crooked* has taken this inference a step further by analyzing expansion and the F-actin cytoskeleton in diverse cell types to provide a global analysis of the role of fine F-actin configurations in allowing localized cell expansion. In addition, the GFP-aided visualization of F-actin organization in *crooked* revealed abnormal regional accumulations of F-actin. As these actin-filled areas did not expand well this observation highlighted yet another facet of actin organization where, in contrast to fine F-actin, dense actin could restrict local growth. The growth aberrations occurred specifically during rapid cell-growth and besides indicating a requirement for the *CROOKED* gene product during rapid growth also implied that a transition from dense actin to loose actin is essential for proper expansion to take place. The observation that small regions in *crooked* cells that managed to expand always displayed relatively fine-F-actin arrays lent support to this conjecture.

Taking these observations together a general picture emerged wherein the differential localization of loose versus dense F-actin could determine the localities where vesicles could be released or retained to promote or restrict expansion. This was tested by predicting intracellular locations in wild type cells where the placement/maintenance of dense actin could direct the way in which a cell could expand (sketches, Fig. 6). Subsequent observations on wild-type cells conformed totally to the predictions (Fig. 6A-D). Our findings are consistent with observations in animal cells (Muallem et al., 1995; Miyake et al., 2001), where a dense actin configuration has been suggested to act as a barrier and hinder the access of vesicles to their target sites. Further support for this F-actin-density-based mechanism has come from our molecular identification of *CROOKED* that implicates an actin polymerization modulating complex hitherto unknown in plants as a pivotal player in the cellular machinery required for creating differential growth conditions.

CROOKED implicates the ARP2/3 complex in actin configurational changes required for localized expansion

CROOKED was found to encode the plant homolog of ARPC5, the smallest subunit of the ARP2/3 complex known from diverse organisms (Machesky et al., 1997; Welch, 1999). A rescue of the mutant phenotype by the human ortholog (Welch et al., 1997) provided strong evidence both for the occurrence and functional conservation of the complex in higher plants. This seven-subunit complex is a highly conserved modulator of actin polymerization (Mullins et al., 1998a; Welch, 1999). Studies in other organisms have shown that it is recruited to sites of dynamic actin assembly, plays a role in actin-polymerization-based membrane protrusion, and in the rocketing motility of vesicles and entero-pathogenic organisms (Welch et al., 1997; Machesky, 1999; Merrifield et al., 1999). The complex enhances F-actin nucleation and side-binding activities to produce a dendritic array of fine actin filaments arising from pre-existing mother filaments (Mullins et al., 1998a; Svitkina and Borisy, 1999). Despite its detailed biochemical and structural characterization (Mullins et al., 1998a; Volkmann et al., 2002) the ARP2/3 complex has not been implicated in cellular morphogenesis in a multicellular

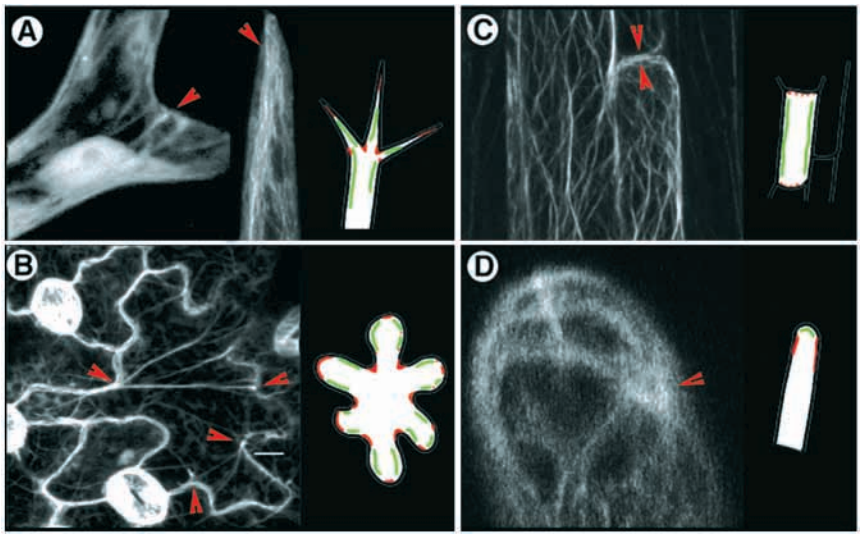

Fig. 6. A simple actin configuration-based model derived through observations of wild-type *Arabidopsis* cells depicts how the strategic placement of dense F-actin (red arrowheads/areas) can restrict local cell expansion, whereas vesicles are free to move out into the assimilation zone and produce expansion in other areas (green) where the F-actin meshwork has been loosened through the activity of the ARP2/3 complex (of which *CROOKED* is an essential component). (A-D) Major locations of dense actin in wild-type *Arabidopsis* cells. (A) Actin accumulations are seen at branch junctions and branch tips in trichome cells. The non-expanding, dense-actin filled tip is projected through the diffuse expansion growth that takes place in the flanks of the extending branches. Non-expansion of the absolute apex in trichomes produces a fine pointed tip. (B) Dense F-actin is found at lobe junctions and in different strategic locations in multi-lobed pavement cells. Contrary to other cell types, the lobes in pavement cells have to constantly adjust to the growth patterns of neighboring cells on all sides. Thus, they may show fluctuations in their dense actin localization, depending upon their position relative to other cells. (C) The elongate, cylindrical hypocotyl cells appear to have dense actin at their ends. Capping of the ends with dense actin reroutes vesicles into the flanking regions. This results is the formation of long cylindrical cells of varying length whose ends maintain a nearly constant diameter. (D) Side view of a blunt tipped growing root-hair cell. The positioning of dense actin bundles changes constantly in an elongating root hair (data not shown) though the general distance from the absolute tip remains almost the same. A dense-actin cap at the tip frequently indicates cessation of hair growth and may lead to swelling behind the actin-blocked tip region. Note that the formation of a pointed tip, as in trichomes, requires a dense actin cap, whereas a broad growing tip requires placement of dense actin at the sides in order to funnel vesicles into the tip region.

eukaryote. The only reported loss-of-function mutant in a higher eukaryote is the ARP3 mutant in *Drosophila*, where defects in ring canal expansion have been observed (Hudson and Cooley, 2002). In single celled yeasts, deletion of the genes encoding individual ARP2/3 complex subunits causes lethality or severe growth disruption (Winter et al., 1999). Our characterization of *crooked* thus provides the first indication that ARP2/3-complex activity is vital for proper cell morphogenesis in higher organisms.

With specific reference to the ARPC5/CROOKED subunit, reconstitution experiments using individual subunits of the complex have suggested that the small subunits ARPC2 (p35), 4(p20) and 5(p16) may be important for the overall integrity of the complex (Gournier et al., 2001). A specific deletion of the ARPC5 subunit led to 85 times less nucleation efficiency of the complex in insect cells (Gournier et al., 2001). Our observations of impaired fine F-actin organization in *crooked* and rescue of the mutant phenotype by the human ortholog suggest that the function of this subunit as a nucleation enhancer may have been conserved across the kingdoms. Alternatively, the small ARPC5 subunit may be required for microfilament bundling because loss of its activity results in actin aggregation and reduced long actin-cable formation (e.g. Fig. 2). Moreover, studies in other organisms have so far not revealed the effects of ARPC5 deletion on the overall actin organization. Though the *crooked* mutant is clearly not a null allele, the non-essential nature of *Arabidopsis* trichomes has allowed the isolation of seven more mutants with distorted trichomes (Hülskamp et al., 1994). Two of these mutants are now known to correspond to ARP2 and ARP3 subunits of the complex and exhibit a similar actin organization as *crooked* (Mathur et al., 2003). Taken together, the mutant phenotypes and the conditional requirement of the complex during rapid growth have allowed the first glimpse of what goes wrong with actin organization in living cells when the actin nucleation-enhancing capability of the ARP2/3 complex is compromised.

ARP2/3 complex mediated actin polymerization may play a role during the vesicle assimilation step

The ARP2/3 complex is best known for its role in the rocketing motility of entero-pathogenic organisms and endocytic vesicles (Machesky, 1999; Merrifield et al., 1999). Specifically, the ARPC5 subunit has been implicated in the motility and distribution of mitochondria in yeast (Boldogh et al., 2001). Although our present observations do not provide evidence for a direct role of *CROOKED* in vesicle motility, it may be speculated that after the release of vesicles into the cortical zone, a certain amount of actin-polymerization generated propulsive force may be required for their effective assimilation into the plasma membrane. The *crooked* mutant may thus be impaired in both vesicle release and assimilation steps.

The molecular identification of *CROOKED* links different regulators of the actin cytoskeleton together

The molecular identification of CROOKED and subsequent demonstration of its functional conservation are strongly suggestive of the occurrence of the ARP2/3 complex in plants and bring together a number of recent observations indicating that some of the key interactors of the complex may already have been identified in plants. For example, from other organisms, the ARP2/3 complex is known to be a downstream target for Rho-like GTPases (Ridley, 2001). In plants, although overexpression of a *ROP* resulted in increased fine F-actin (Fu et al., 2002) the identity of the downstream effector was so far

unclear. Similarly, mutations in the novel maize *BRICK1* gene show actin cytoskeleton linked defects including an inability to form epidermal lobes and differentiate stomatal complexes (Frank and Smith, 2002). A human homolog of *BRICK1*, the *HSPC300* gene, has been shown to interact with the ARP2/3 complex (Eden et al., 2002; Smith, 2003), whereas two additional BRICK genes are speculated to be ARP2/3 complex activators (Frank et al., 2003) similar to the WASP family activators in animal systems (Higgs and Pollard, 2001). The molecular link provided by the cloning of *CROOKED* suggests that the mechanism for actin modulation involving the *ROP* and *BRK* genes, and the ARP2/3 complex may be well conserved between plants and other organisms. The complex is also known to interact with profilins (Mullins et al., 1998b), actin-depolymerizing-factors (ADF/cofilin) (Svitkina and Borisy, 1999), which along with different F-actin bundling proteins are already known to share the same intracellular domains in expanding plant cells (Jiang et al., 1997; Dong et al., 2001; Vidali et al., 2001; Vantard and Blanchoin, 2002). Finally, although not addressed here, the *crooked* mutant provides an enviable tool to understand the interactions between the actin and microtubular components of the cytoskeleton in higher plants, including their apparent cooperative roles in subcellular motility and cell morphogenesis.

Conclusions

The following generalizations on cell-shape development have emerged from the cell-biological/molecular characterization of *CROOKED*: (1) fine F-actin, generated through the mediation of the ARP2/3 complex (where the ARPC5/CROOKED subunit plays an important role in maintaining the complex-nucleating capability), is required for cell expansion to occur; (2) a localized increase in the presence of organelles and vesicles at a spot does not necessarily translate into localized expansion, rather expansion can proceed only when vesicles carrying cell-building material can be released and assimilated; and (3) the spatiotemporal regulation of F-actin density within a cell can create a loose sieve to allow vesicle release or a dense barrier to trap vesicles and thus determine where and when vesicles will be released for effective local expansion; The cumulative result from these phenomenon can account for the diverse cell shapes observed in plants (Fig. 6).

We thank Prof. C. Hawes (Oxford Brookes University, Oxford) for the ERD2-GFP construct; Prof. S. Craig (John Hopkins University School of Medicine, Baltimore) for the mouse Talin gene; Dr M. Welch (University of California, Berkeley) for the human ARPC5 cDNA; Prof. N.-H. Chua (Rockefeller University, New York) for GFP-mTalin transgenic *Arabidopsis*; Prof. D. Tautz (University of Köln) for allowing use of the Leica Confocal and the ABI sequencing facilities; Prof. P. J. Hussey (University of Durham) and Prof. C.W. Lloyd (John Innes Centre, Norwich) for their comments and guidance on the manuscript; and Anshudeep Mathur for help with graphics and computer work. The study was supported by a Volkswagen Stiftung grant to M.H.

REFERENCES

Altschul, S. F., Madden, T. L., Schaffer, A. A., Zhang, J., Zhang, Z., Miller, W. and Lipman, D. J. (1997). Gapped BLAST and PSI-BLAST: a new generation of protein database search programs. *Nucleic Acids Res.* **25**, 3389-3402.

Baluska, F., Jasik, J., Edelmann, H. G., Salajova, T. and Volkmann, D. (2001). Latrunculin-B induced plant dwarfism: plant cell elongation is F-actin dependent. *Dev. Biol.* **231**, 618-632.

Boevink, P., Oparka, K., Santa Cruz, S., Martin, B., Betteridge, A. and Hawes, C. (1998). Stacks on tracks: the plant Golgi apparatus traffics on an actin/ ER network. *Plant J.* **15**, 441-447.

Boldogh, I. R., Hyeong-Cheol, L., Nowakowski, W. D., Karmon, S. L., Hays, L. G., Yates, J. R., III and Pon, L. A. (2001). ARP2/3 complex and actin dynamics are required for actin-based mitochondrial motility in yeast. *Proc. Natl. Acad. Sci. USA* **98**, 3162-3167.

Clough, S. J. and Bent, A. F. (1998). Floral dip: a simplified method for *Agrobacterium*-mediated transformation of *Arabidopsis thaliana*. *Plant J.* **16**, 735-743.

Cooper, J. A., Wear, M. A. and Weaver, A. M. (2001). ARP2/3 complex: advances on the inner workings of a molecular machine. *Cell* **107**, 703-705.

Dong, C. H., Kost, B., Xia, G. and Chua, N.-H. (2001). Molecular identification and characterization of the *Arabidopsis AtADF1, AtADF5* and *ATADF6* genes. *Plant Mol. Biol.* **45**, 517-527.

Eden, S., Rohtagi, R., Podtelejnikov, A. V., Mann, M. and Kirschner, M. W. (2002). Mechanism of regulation of WAVE1-induced actin nucleation by Rac1 and Nck. *Nature* **418**, 790-793.

Foissner, I., Lichtscheidl, I. K. and Wasteneys, G. O. (1996). Actin-based vesicle dynamics and exocytosis during wound wall formation in Characean internodal cells. *Cell. Motil. Cytoskeleton* **35**, 35-48.

Frank, M. J. and Smith, L. G. (2002). A small, novel protein highly conserved in plants and animals promotes the polarized growth and division of maize leaf epidermal cells. *Curr. Biol.* **12**, 849-853.

Frank, M. J., Cartwright, H. N. and Smith, L. G. (2003). Three Brick genes have distinct functions in a common pathway promoting polarized cell division and cell morphogenesis in the maize leaf epidermis. *Development* **130**, 753-762.

Fu, Y., Li, H. and Yang, Z. (2002). The ROP2 GTPase controls the formation of cortical fine F-actin and the early phase of directional cell expansion during *Arabidopsis* organogenesis. *Plant Cell* **14**, 777-794.

Geitmann, A. and Emons, A. M. (2000). The cytoskeleton in plant and fungal cell tip growth. *J. Microsc.* **198**, 218-245.

Gournier, H., Goley, E. D., Niederstrasser, H., Trinh, T. and Welch, M. D. (2001). Reconstitution of human Arp2/3 complex reveals critical roles of individual subunits in complex structure and activity, *Mol. Cell.* **8**, 1041-1052.

Hawes, C. R., Brandizzi, F. and Andreeva, A. V. (1999). Endomembranes and vesicle trafficking. *Curr. Opin. Plant Biol.* **2**, 454-461.

Hepler, P. K., Vidali, L. and Cheung, A. Y. (2001). Polarized cell growth in higher plants. *Annu. Rev. Cell Dev. Biol.* **17**, 159-187.

Higgs, H. N. and Pollard, T. D. (2001). Regulation of actin filament network formation through Arp2/3 complex: activation by a diverse array of proteins. *Annu. Rev. Biochem.* **70**, 649-676.

Hudson, A. M. and Cooley, L. (2002). A subset of dynamic actin rearrangements in *Drosophila* requires the ARP2/3 complex. *J. Cell Biol.* **156**, 677-668.

Hülskamp, M., Misera, S. and Jürgens, G. (1994). Genetic dissection of trichome cell development in *Arabidopsis*. *Cell* **76**, 555-566.

Jiang, C. J., Weeds, A. G. and Hussey, P. J. (1997). The maize actin-depolymerizing-factor, ZmADF3, redistributes to the growing tip of elongating root hairs and can be induced to translocate into the nucleus with actin. *Plant J.* **12**, 1035-1043.

Ketelaar, T., de Ruijter, N. C. A. and Emons, A. M. C. (2003). Unstable F-actin specifies the area and microtubule direction of cell expansion in *Arabidopsis* root hairs. *Plant Cell.* **15**, 285-292.

Kost, B., Spielhofer, P. and Chua, N.-H. (1998). A GFP-mouse talin fusion protein labels plant actin filaments in vivo and visualizes the actin cytoskeleton in growing pollen tubes. *Plant J.* **16**, 393-401.

Kost, B., Spielhofer, P., Mathur, J., Dong, C. H. and Chua, N.-H. (2000). Non-invasive F-actin visualization in living plant cells using a GFP-mouse talin fusion protein. In *Actin: A Dynamic Framework for Multiple Plant Cell Functions* (ed. C. J. Staiger, F. Baluska, D. Volkmann and P. W. Barlow), pp. 637-659. Dordrecht: Kluwer Academic.

Machesky, L. (1999). Rocket-based motility: A universal mechanism? *Nat. Cell. Biol.* **1**, E29-E31.

Machesky, L. M. and Gould, K. L. (1999). The ARP2/3 complex: a multifunctional actin organizer. *Curr. Opin. Cell Biol.* **11**, 117-121.

Machesky, L. M., Reeves, E., Wientjes, F., Mattheyse, F. J., Grogan, A., Totty, N. F., Burlingame, A. L., Hsuan, J. J. and Segal, A. W. (1997). Mammalian actin-related protein 2/3 complex localizes to regions of

lamellipodia protrusion and is composed of evolutionary conserved proteins. *Biochem. J.* **328**, 105-112.

Mathur, J. and Koncz, C. (1997). Method for Preparation of Epidermal Imprints using agarose. *Biotechniques* **22**, 280-282.

Mathur, J., Spielhofer, P., Kost, B. and Chua, N. H. (1999). The actin cytoskeleton is required to elaborate and maintain spatial patterning during trichome cell morphogenesis in *Arabidopsis thaliana. Development* **126**, 5559-5568.

Mathur, J., Mathur, N. and Hülskamp, M. (2002). Simultaneous visualization of peroxisome and cytoskeletal elements reveals actin and not microtubule-based peroxisome motility in plants. *Plant Physiol.* **128**, 1031-1045.

Mathur, J. and Hülskamp, M. (2002). Microtubules and microfilaments in cell morphogenesis in higher plants. *Curr. Biol.* **12**, R669-R676.

Mathur, J., Mathur, N., Kernebeck, B. and Hulskamp, M. (2003). Mutations in Actin Related Proteins 2 and 3 affect cell shape development in *Arabidopsis thaliana*. *Plant Cell* (in press).

McKann, R. O. and Craig, S. W. (1997). The I/LWEQ module: A conserved sequence that signifies F-actin binding in functionally diverse proteins from yeast to mammals. *Proc. Natl. Acad. Sci. USA* **94**, 5679-5684.

Merrifield, C. J., Moss, S. E., Ballestrem, C., Imhof, B. A., Giese, G., Wunderlich, I. and Almers, W. (1999). Endocytic vesicles move at the tips of actin tails in cultured mast cells. *Nat. Cell Biol.* **1**, 72-74

Miller, D. D., de Ruitjer, N. C. A., Bisseling, T. and Emons, A. M. C. (1999). the role of actin in root hair morphogenesis: studies with lipochito-oligosaccharide as a growth stimulator and cytochalasin as an actin perturbing drug. *Plant J.* **17**, 141-154.

Miyake, K., McNeil, P. l., Suzuki, K., Tsunoda, R. and Sugai, N. (2001). An actin barrier to resealing. *J. Cell Sci.* **114**, 3487-3492.

Muallem, S., Kwiatkowska, K., Xu, X. and Lin, H. L. (1995). Actin filament disassembly is a sufficient final trigger for exocytosis in non-excitable cells. *J. Cell Biol.* **128**, 589-598.

Mullins, R. D., Heuser, J. A. and Pollard, T. D. (1998a). The interaction of Arp2/3 complex with actin: Nucleation, high affinity pointed end capping, and formation of branching networks of filaments. *Proc. Natl. Acad. Sci. USA* **95**, 6181-6186.

Mullins, R. D., Kelleher, J. F., Xu, J. and Pollard, T. D. (1998b). Arp2/3 complex from Acanthamoeba binds profilin and cross-links actin filaments. *Mol. Biol. Cell* **9**, 841-852.

Murashige, T. and Skoog, F. (1962). A revised medium for rapid growth and bioassays with tobacco tissue cultures. *Physiol. Plant* **15**, 473-497.

Nebenführ, A., Gallagher, L. A., Dunahay, T. G., Frohlick, J., Mazurkiewicz, A. M., Meehl, J. B. and Staehelin, A. L. (1999). Stop-and-go movements of plant golgi stacks are mediated by actin- myosin system. *Plant Physiol.* **121**, 1127-1141.

Qualmann, B., Kessels, M. M. and Kelly, R. B. (2000). Molecular links between endocytosis and the actin cytoskleton. *J. Cell Biol.* **150**, F111-F116.

Ridley, A. J. (2001). Rho proteins: linking signaling with mmbrane trafficking. *Traffic* **2**, 303-310.

Sambrook, J. and Russell, D. W. (2001). *Molecular Cloning. A Laboratory Manual*. Cold Spring Harbor, New York: Cold Spring Harbor Laboratory Press.

Smith, L. G. (2003). Cytoskeletal control of plant cell shape: getting the fine points. *Curr. Opin. Plant Biol.* **6**, 63-73.

Svitkina, T. M. and Borisy, G. G. (1999). ARP2/3 complex and actin depolymerizing factor/cofilin in dendritic organization and treadmilling of actin filament array in lamellipodia. *J. Cell Biol.* **145**, 1009-1026.

Szymanski, D. B., Jilk, R. A., Pollock, S. M. and Marks, M. D. (1998). Control of GL2 expression in *Arabidopsis* leaves and trichomes. *Development* **125**, 1161-1171.

Szymanski, D. B., Marks, D. M. and Wick, S. M. (1999). Organized F-actin is essential for normal trichome morphogenesis in *Arabidopsis. Plant Cell* **11**, 2331-2347.

Vantard, M. and Blanchoin, L. (2002). Actin polymerization processes in plant cells. *Curr. Opin. Plant Biol.* **5**, 502-506.

Vidali, L., Mckenna, S. T. and Hepler, P. K. (2001). Actin polymerization is essential for pollen tube growth. *Mol. Biol. Cell* **12**, 2534-2545.

Volkmann, N., Amann, K. J., Stoilova-McPhie, S., Egile, C., Winter, D. C., Hazelwood, L., Heuser, J. E., Li, R., Pollard, T. D. and Hanein, D. (2001). Structure of Arp2/3 complex in its activated state and in actin filament branch junctions. *Science* **293**, 2456-2459.

Welch, M. D., DePace, A. H., Verma, S., Iwamatsu, A. and Mitchison, T. J. (1997). The human ARP2/3 complex is composed of evolutionary conserved subunits and is localized to cellular regions of dynamic actin filament assembly. *J. Cell Biol.* **138**, 375-384.

Welch, M. D. (1999). The world according to Arp: regulation of actin nucleation by the Arp2/3 complex. *Trends Cell Biol.* **9**, 423-427.

Williamson, R. E. (1993). Organelle movements. *Annu. Rev. Plant Physiol. Plant Mol. Biol.* **44**, 181-202.

Winter, D. C., Choe, E. Y. and Li, R. (1999). Genetic dissection of the budding yeast ARP2/3 complex: a comparison of the in vivo and structural roles of individual subunits. *Proc. Natl. Acad. Sci. USA* **96**, 7288-7293.